

Electron localization and interaction effects in thin antimony films

A. V. Butenko and E. I. Bukhshtab

Physicotechnical Institute of Low Temperatures, Ukrainian Academy of Sciences

(Submitted 3 September 1984)

Zh. Eksp. Teor. Fiz. **88**, 1053–1063 (March 1985)

We investigate electron localization and interaction effects, which yield information on electron-scattering processes, in antimony films 85–120 Å thick in magnetic fields up to 17 kOe at liquid helium and hydrogen temperatures. The temperature and magnetic-field dependences of the film conductivity are explained by the theory of weak localization and electron-electron interaction in quasi-two-dimensional systems. Values are obtained for the elastic relaxation time τ , the electron-wave-function phase relaxation time τ_φ which is connected with the inelastic and spin-spin (τ_s) scattering processes, and the relaxation time τ_{so} for the spin-orbit interaction. Possible electron-scattering mechanisms are discussed, viz., electron-electron at $T = 1.5$ – 4.2 K and electron-phonon at $T = 14$ – 20 K.

Studies^{1–4} of the electric properties of thin bismuth and antimony films at low temperatures revealed a number of irregularities that were unexplained until the early 80's. These included the low-temperature minimum in the temperature dependence of the resistance and the anomalous magnetoresistance. Advances in the theory^{5,6} made it possible to attribute these irregularities to weak localization (WL) effects and to electron-electron interaction (EEI). In particular, a series of experiments on bismuth^{7–10} explained fully all the anomalies observed and reconciled them with the WL and EEI theory.

Anomalies in the temperature and magnetic-field dependences of the electric resistance of antimony films are also due to WL and EEI effects.¹¹ We report here the results of a detailed investigation of the electric properties of thin (80–100 Å) antimony films at liquid helium and hydrogen temperatures in magnetic fields up to 17 kOe, which permits an assessment of the roles of various electron-scattering processes.

Let us dwell briefly on the predictions of the WL and EEI theory which were compared with the experimental results of this study.

The temperature dependence of the film-conductivity increment due to WL and EEI effects is described for the two-dimensional case with strong spin-orbit interaction¹⁾ by the expression

$$\Delta\sigma_\tau = \left(-\frac{1}{2}p + \lambda \right) \frac{e^2}{2\pi^2\hbar} \ln T\tau = a \cdot \frac{e^2}{2\pi^2\hbar} \ln T\tau, \quad (1)$$

where σ is the conductivity of the film (here and below R and σ are the resistance and conductivity of a square film), τ is the total electron relaxation time, p is the exponent in the expression $\tau_\varphi \sim T^{-p}$, τ_φ is the wave-function relaxation time, and λ is the electron-electron interaction constant for electrons with small momentum difference (diffusion channel). The term that takes into account for the EEI for electrons with a small momentum sum (the Cooper channel) and the Maki-Thompson correction⁵ will be neglected, since these are small.¹¹

The wave-function in phase-relaxation time consists of two terms

$$\tau_\varphi^{-1} = \tau_{in}^{-1} + 2\tau_s^{-1}, \quad (2)$$

where τ_{in} is the relaxation time for inelastic scattering processes and τ_s is the spin-spin relaxation time.

In a classically weak magnetic field the WL effects are annihilated, but the EEI in the diffusion channel remains unchanged. This is how the WL and EEI effects in the temperature dependence of $\Delta\sigma$ in bismuth films were separated in Ref. 9, where the values $p \approx 1$ and $\lambda \approx 1$ were obtained.

Abundant information on the WL and EEI effects is obtained by measuring the magnetic-field dependence of the films in magnetic fields perpendicular and parallel to the surface. Theory yields the following expression for the $\Delta\sigma(H)$ dependence:

$$\Delta\sigma(H_\perp) = \frac{e^2}{2\pi^2\hbar} \left[-\frac{1}{2} f_2 \left(\frac{4eDH}{\hbar c} \tau_\varphi \right) + \frac{3}{2} f_2 \left(\frac{4eDH}{\hbar c} \tau_\varphi^* \right) \right], \quad (3)$$

$$\Delta\sigma(H_\parallel) = \frac{e^2}{2\pi^2\hbar} \left[-\frac{1}{2} \ln \left(\frac{\tau_\varphi}{\tau_{H_\parallel}} + 1 \right) + \frac{3}{2} \ln \left(\frac{\tau_\varphi^*}{\tau_{H_\parallel}} + 1 \right) \right], \quad (4)$$

where D is the electron-diffusion coefficient, $(\tau_\varphi^*)^{-1} = \tau_\varphi^{-1} + \frac{4}{3}\tau_{so}^{-1}$, τ_{so} is the spin relaxation time due to the spin-orbit interaction in elastic scattering of the electrons, $\tau_{H_\parallel}^{-1} = L^2 e^2 H^2 D / 3\hbar^2 c^2$; $f_2(x) = \ln x + \psi(\frac{1}{2} + 1/x)$, and ψ is the digamma function.

If $\tau_{so} \ll \tau_\varphi$ the first terms dominate in Eqs. (3) and (4) and determine the anomalous positive magnetoresistance, since the term with τ^* is small in fields up to 17 kOe. This case was observed in measurements of the magnetoconductance of bismuth^{7–10} and antimony¹¹ films, where the $\Delta\sigma(H)$ relations were well described by expressions (3) and (4): in weak fields the experimental curves coincide with the first term, and in strong fields the contribution of the second term is significant and permits an estimate of τ_{so} .

SAMPLES AND EXPERIMENT

Our measurements were performed on polycrystalline antimony films 85–150 Å thick obtained by condensation, in a vacuum of 10^{-7} Torr on glass substrates at room temperature. The thickness was monitored during the deposition with a quartz oscillator, and the distribution of the film thickness along a wedge-shaped sample was determined in-

dependently. The error in the absolute thickness was less than 10%, and the relative error in the thicknesses of the neighboring sections was negligible ($\leq 10^{-2}$).

The antimony is condensed on a room-temperature substrate initially as an amorphous phase. Once the critical thickness is reached (the minimum thickness of the conducting film, ~ 80 Å in our case), crystallization sets in and spreads from the thicker to the thinner region. The amorphous antimony crystallizes via the onset and growth of spherulites, which are polycrystalline formations with radially projecting structure: the (111) plane of the crystallite is parallel to the film surface. At large thickness (noticeably above critical) the crystalline antimony layer is made highly regular by the presence of a texture, by the relatively small disorientation angles between the adjacent crystallites, and by the relatively large size of the latter ($\approx 10^{-5}$ cm). The high degree of disorder needed to study the localization effect was therefore achieved in the thinnest conducting samples, of thickness $L = 85\text{--}100$ Å.

The sample resistance varied smoothly from $\sim 2 \cdot 10^3$ Ω for the thinnest to $\sim 1.4 \cdot 10^2$ Ω for the thickest films investigated. The temperature was varied in the ranges 1.4–4.2 K (helium region) and 14–20 K (hydrogen region). The samples were placed directly in the liquid. A magnetic field up to 17 kOe was produced by an external electromagnet and was directed perpendicular or parallel to the plane of the film, accurate to within $< 1^\circ$. The measurements were made by the four-contact method using a 10-μA dc current. The low measuring current prevented heating. The current-voltage characteristic was checked: Ohm's law held in fields suitable for the measurements. The magnetic-field dependences were recorded on an automatic x - y potentiometer accurate to $\sim 1\%$.

TEMPERATURE DEPENDENCE OF THE CONDUCTIVITY

The temperature dependence of the electric conductivity of thin antimony films reveals a low-temperature resistance minimum and an increase of the resistance with decreasing temperature.⁴ Compared with bismuth films,^{7–10} the antimony film produced had a higher resistance, so that the WL and EEI effects could be observed at higher temperatures (14–20 K).

The low-temperature increase of the conductivity in a magnetic field (and the absence of a field) satisfies expression (1) of the WL and EEI theory (Fig. 1).

The inset of Fig. 2 shows the dependence of the slope of the $\Delta\sigma_T(\ln T)$ curves in the helium and hydrogen temperature regions, which is equal to the coefficient a^* preceding the logarithm in (1).

A simple method can be proposed to determine the exponent p from the temperature dependence of the magnetoconductance in a weak magnetic field parallel to the film plane. In accordance with (4) we have at $\tau_\varphi/\tau H_{||} \ll 1$

$$\Delta\sigma(H_{||}) = -\frac{1}{2} \frac{e^2}{2\pi^2\hbar} \frac{L^2 e^2 H^2 D}{3\hbar^2 c^2} \tau_\varphi \quad (5)$$

and if $\tau_\varphi \propto T^{-p}$ the slope of the plot of $\ln\Delta\sigma$ vs $\ln T$ in a fixed magnetic field is proportional to p (D is independent of temperature). Figure 2 shows the experimental plots of $\ln\Delta\sigma$ vs

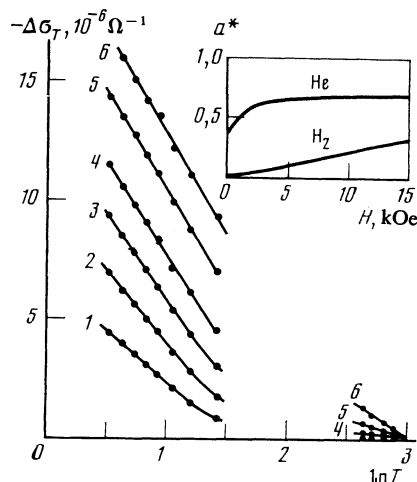


FIG. 1. Quantum correction to the conductivity of an antimony film 89 Å thick as a function of temperature in various magnetic fields: $H = 0$ (curve 1); 1.1 (2); 2.3 (3); 3.9 (4); 7.6 (5); 13.6 kOe (6). Inset—dependence of the coefficient a^* in (1) on the magnetic field in the helium and hydrogen temperature ranges.

$\ln T$ in various fields ($H < 3000$ Oe); they are straight lines with a slope $p = 1$ that does not depend on H .

A value $p = 1$ was also obtained in Ref. 11 and in the analysis below of the magnetic-field dependence of antimony films (at $t = 1.5\text{--}4.2$ K). In conjunction with the data of Fig. 1 this yields a value $\lambda \approx 0.85$ for the electron-electron interaction constant in the diffusion channel.

In the helium region and in strong magnetic field the coefficient a^* in Fig. 1 tends to a value ≈ 0.7 ($a^* = \lambda$ for sufficiently high H). At temperatures 14–20 K in the absence of a field we have $p \approx 1.7$ and $a^* = 0$, with the same value $\lambda \approx 0.85$; a^* increase in a magnetic field, but only to $a^* \approx 0.3$, since the characteristic fields for the localization effect increase strongly at these temperatures (see Table I) and in the fields we used up to 17 kOe, the localization effects persist.

CHANGE OF CONDUCTIVITY IN A MAGNETIC FIELD

When the samples are placed in a magnetic field parallel or perpendicular to the film plane, an anomalous positive magnetoresistance is observed (Fig. 3) which depends on the temperature and on the film thickness. This dependence of L

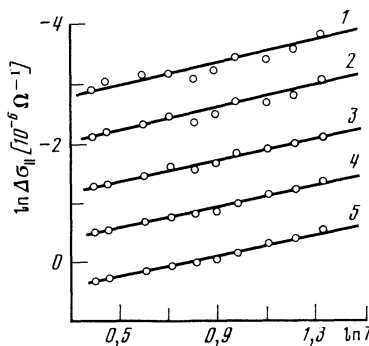


FIG. 2. Temperature dependence of the magnetoconductance in weak magnetic fields parallel to the plane of the Sb film: $H = 545$ (curve 1), 820 (2), 1270 (3), 1910 (4), 3000 Oe (5); $L = 89$ Å.

TABLE I. Values of the characteristic fields for the localization and interaction effects: Sb sample, $L = 85 \text{ \AA}$, $D = 2.4 \text{ cm}^2/\text{s}$.

$T, \text{ K}$	1,5	4,2	20
$D\tau_\varphi, 10^{-10} \text{ cm}^2$	0,68	0,28	0,05
$H_\perp^{0 \text{ loc}} = \hbar c/4eD\tau_\varphi, \text{ Oe}$	244	593	3 300
$H_\perp^{0 \text{ int}} = \pi ckT/2eD, \text{ Oe}$	8 120	22 700	110 000
$H_\parallel^{0 \text{ loc}} = \frac{3^{1/2}\hbar c}{eL(D\tau_\varphi)^{1/2}}, \text{ Oe}$	16 000	25 000	60 000
$H_\parallel^{0 \text{ int}} = \frac{3^{1/2}\hbar c}{eL} \left(\frac{kT}{\hbar D} \right)^{1/2}, \text{ Oe}$	38 000	63 000	139 000

and T is connected with the $\tau_\varphi(T, L)$ and $D(L)$ dependences in Eqs. (3) and (4).

In weak fields ($H_\perp < \hbar c/4eD\tau_\varphi = H_\perp^0$ and $H_\parallel < 3^{1/2}\hbar c/Le(D\tau_\varphi)^{1/2} = H_\parallel^0$); the quantum interference corrections are proportional to H^2 , with the quadratic region considerably wider in a parallel field than in a perpendicular one. The characteristic fields for the localization and interaction effects, calculated from (3) and (4), are listed in Table I.

As the temperature is lowered the time τ_φ increases, which leads to a decrease of the region of the quadratic relation $\Delta\sigma \propto H^2$. The slope of the $\Delta\sigma(H_\parallel^0)$ plot is proportional to the phase-relaxation time τ_φ and increase with decreasing temperature.

In a perpendicular magnetic field the region $\Delta\sigma \propto H^2$ is much narrower (10^2 Oe) at helium temperatures, but increases strongly with rising temperature, so that the characteristic fields $H_\perp^0 \propto 1/\tau_\varphi$ (whereas $H_\parallel^0 \propto \tau_\varphi^{-1/2}$)

$$\Delta\sigma(H_\perp) = -\frac{1}{48} \frac{e^2}{2\pi^2\hbar} \left(\frac{4eD\tau_\varphi}{\hbar c} \right)^2 H^2, \quad H < H_\perp^0. \quad (6)$$

In strong magnetic field the quantum interference corrections $\Delta\sigma$ tend to become proportional to $\ln H$, but it is possible to dispense with the asymptotic forms and compare the experimental $\Delta\sigma(H)$ to the theoretical ones in all mea-

sured fields. Figure 4 shows such a comparison of $\Delta\sigma(H_\perp)$ with Eq. (3). The experimental $\Delta\sigma(\ln H_\perp)$ curves match the calculated plot of

$$-\frac{1}{2} \frac{e^2}{2\pi^2\hbar} f_2(\ln x)$$

without any adjustable parameters whatever; superposition, on the abscissa, of the scales of $\ln H$ and

$$\ln x = \ln H + \ln D\tau_\varphi + \text{const}$$

determines the value of $D\tau_\varphi$.

The experimental curves of Fig. 4 agree with those calculated in fields $H \lesssim 10 \text{ kOe}$. In stronger magnetic fields a deviation is observed resulting from the positive contribution made to $\Delta\sigma$ by the second term of (3). From this deviation we can estimate the time τ_{so} , which was found to be $\approx 5 \cdot 10^{-13} \text{ s}$, i.e., much shorter than $\tau_\varphi \approx 10^{-11} \text{ s}$.

To determine τ_φ from the experimentally obtained values of $D\tau_\varphi$ we must know the diffusion coefficient, which can be calculated from the formula $D = (1.3)v_F^2 \tau$, where τ is the total relaxation time in the expression $\sigma = ne^2\tau/m^*$. The values of m^* , n , and v_F for this calculation were taken from Refs. 12 and 13. The resulting values of D , as well as other measured and calculated parameters of the investigated antimony films, are listed in Table II.

The experimental phase-relaxation lengths $L_\varphi = (D\tau_\varphi)^{1/2}$ are evidence that $L_\varphi > L$ for all the films at $T = 4.2 \text{ K}$. L_φ is at least twice as large as L even at 20 K . The condition $L_H > L$ is satisfied in the fields $H < 17 \text{ kOe}$ used in the present paper. With increasing temperature, the length $L_T = (\hbar D/kT)^{1/2}$ that characterizes the interaction effects decreases, and at $T = 20 \text{ K}$ we have $L_T \gtrsim L$ for the thinnest sample. In thicker films, the condition $L_T > L$ is well satisfied. (D increases rapidly with increasing L .) Thus, the conditions $L < L_\varphi, L_T, L_H$ that the localization and interaction effects be two-dimensional are satisfied at all fields and temperatures used in the experiment.

The EEI effects manifest themselves in the diffusion channel by a temperature dependence of the resistance, while the magnetic-field dependences are connected only with weak-localization effects, since the characteristic fields needed to observe the EEI contribution are much stronger (Table I).

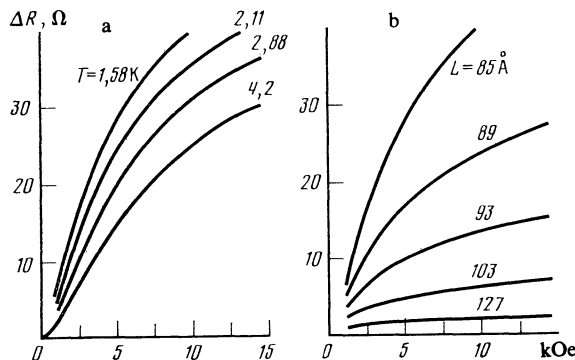


FIG. 3. Typical plots of antimony-film magnetoresistance in a perpendicular magnetic field: a—at various temperatures, $L = 89 \text{ \AA}$; b—for various film thicknesses, $T = 4.2 \text{ K}$; the abscissa is $\ln H_\perp$.

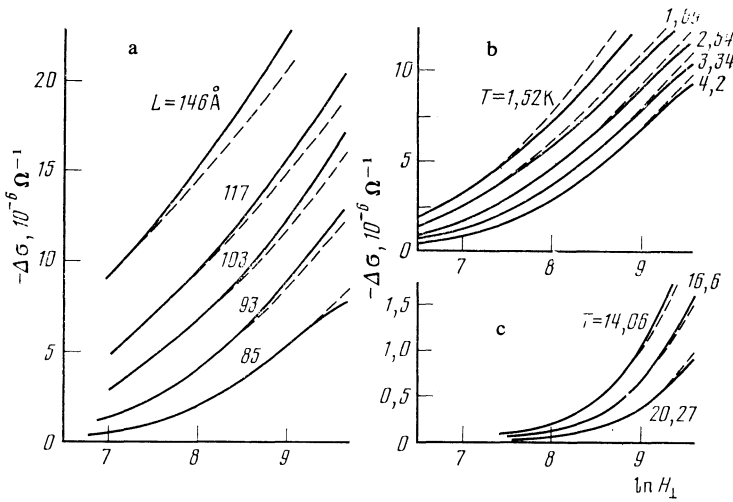


FIG. 4. Comparison of field dependence of the magnetoconductance with the theory [Eq. (3)] at $T = 4.2$ K for various film thicknesses (a) and at $L = 89$ Å for various temperatures (b, c). Solid curves—experiment, dashed—the function $\frac{1}{2}(e^2/2\pi^2\hbar)f_2(x)$. Superposition of the $\ln H$ and $\ln x$ axes determines the value of $D\tau_\varphi$.

POSSIBLE MECHANISMS OF ELECTRON INELASTIC RELAXATION

Measurements of the WL effects in a magnetic field have made it possible to determine experimentally the wavefunction phase-relaxation time τ_φ which is connected with the inelastic processes in the electron system.

The value of τ_φ varies with temperature and with film thickness. $\tau_\varphi \propto T^{-1}$ in the helium region 1.5–4.2 K and $\tau_\varphi \propto T^{-p}$ at 14–20 K, where $p = 1.7$ –2. The apparent reason is that the principal mechanism of inelastic electron scattering changes with temperature.²⁾

The plots of τ_φ^{-1} vs T at 1.5–4.2 K are straight lines that do not pass through the origin (Fig. 5), i.e., in accordance with (2), τ_φ contains as terms the inelastic time τ_{in} and the spin-spin relaxation time τ_s . The values of τ_s are $2.2 \cdot 10^{-10}$ and $\sim 3 \cdot 10^{-10}$ s for samples with $L = 85$ and 89 Å, respectively, i.e., they exceed τ_φ by more than a factor of ten.

No contribution of τ_s was observed in thicker samples. The characteristic length $L_s = (D\tau_s)^{1/2}$ amounts to $\sim 2 \cdot 10^{-5}$ cm ($L = 85$ Å) and $\sim 3 \cdot 10^{-5}$ cm ($L = 89$ Å), thus substantially exceeding τ_φ , and is of the same order as the crystallite size.

It can be assumed that the spins are scattered by amorphous-phase microinclusions in the intercrystallite boundaries or in the voids that can exist in films of near-critical thickness. Such minute inclusions with fully developed amorphous—crystalline phase interface or amorphous phase—vacuum interface can locally contain uncompensated spins that serve as spin-scattering centers. As the film thickness increases away from the critical value, the number of these voids in the film decreases rapidly, and therefore no τ_s contribution is observed for samples with $L > 90$ Å.

The relation $\tau_\varphi \propto T^{-1}$ at helium temperatures should be attributed (as in bismuth) to electron-electron interaction enhanced by the diffuse character of the electron motion as a result of strong impurity scattering.¹⁴ The theory of EEI in disordered systems yields in the two-dimensional case the following expression for the phase-relaxation time τ_φ due to electron-electron collisions with small momentum transfer:

$$\tau_\varphi^{-1} = \frac{\pi k T}{\hbar} \frac{R e^2}{2\pi^2 \hbar} \ln \frac{\pi \hbar}{e^2 R}. \quad (7)$$

The experimental results agree well with the values calculated from Eq. (7) (Table II); the temperature dependence at $T < 4.2$ K also agrees with the theory.

TABLE II. Properties of investigated samples. Measured and calculated values of parameters typical of the localization effect at $T = 4.2$ K.

L , Å	85	89	93	98	
R , Ω	1833,2	1281,5	857,6	610,3	
D , cm/s	2,50	3,50	5,14	7,08	
τ , 10^{-14} s	0,41	0,57	0,84	1,15	
$\tau_\varphi^{\text{exp}}$, 10^{-11} s	1,00	1,02	1,03	1,04	
L_φ , 10^{-5} cm	0,49	0,57	0,68	0,84	
$\tau_\varphi^{\text{calc}}$, 10^{-11} s [14]	1,31	1,59	2,02	2,53	
τ_{ee}^{calc} , 10^{-11} s [15]	0,020	0,026	0,036	0,046	
L , Å	103	108	113	117	121
R , Ω	517,3	424,5	382,5	327,0	295,3
D , cm/s	8,40	9,73	10,5	12,1	13,1
τ , 10^{-14} s	1,33	1,59	1,71	1,98	2,14
$\tau_\varphi^{\text{exp}}$, 10^{-11} s	1,08	1,22	1,27	1,31	1,49
L_φ , 10^{-5} cm	0,95	1,09	1,15	1,26	1,40
$\tau_\varphi^{\text{calc}}$, 10^{-11} s [14]	2,83	3,25	3,50	3,92	4,22
τ_{ee}^{calc} , 10^{-11} s [15]	0,054	0,060	0,064	0,072	0,077

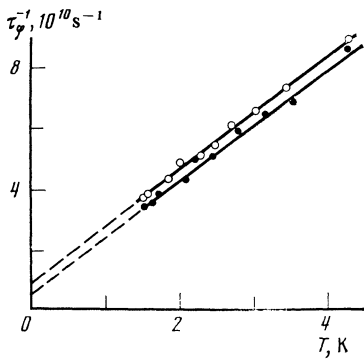


FIG. 5. Dependence of τ_φ^{-1} on T for antimony films 85 Å (○) and 89 Å (●) thick.

Table II lists also the electron-electron relaxation times calculated from an equation given in Ref. 15:

$$\tau_{ee}^{-1} = \frac{kT}{2Dm} \ln \frac{T_1}{T}, \quad kT_1 = \frac{32}{27} (k_F l)^3 \text{ Ry} \quad (8)$$

(m is the effective mass, k_F is the Fermi wave momentum of the electron, l is the mean free path, and Ry is the Rydberg unit). The values of τ_{ee} calculated from (8) are lower by almost two decades than the experimental τ_φ ; this is perfectly natural, since the time between collisions was calculated in Ref. 15 without considering how small the ensuring phase shift may be.

It was also possible to estimate from the experimental data the spin-orbit interaction time τ_{so} for elastic scattering in antimony films ($\tau_{so} \approx 5 \cdot 10^{-13}$ s). The small value of the term which contains τ_{so} in (3) does not permit a more accurate calculation of τ_{so} and a determination of its thickness dependence.

A plot of the time τ_φ vs film thickness is shown in Fig. 6. At $T < 4.2$ K, τ_φ increases with increasing L , as follows from Eq. (7) for the EEI ($\tau_\varphi \sim 1/R$, R decreases with increasing L). At hydrogen temperatures the $\tau_\varphi(L)$ dependence is inverted. This can be evidence that a change takes place in the principal mechanism of inelastic relaxation of the electrons.

The relaxation time of electron-electron interaction accompanied by large momentum transfer is described by the familiar expression

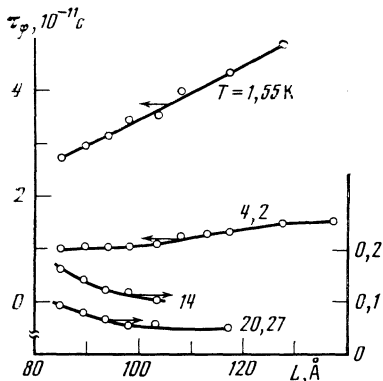


FIG. 6. Dependence of τ_φ on the film thickness at various temperatures.

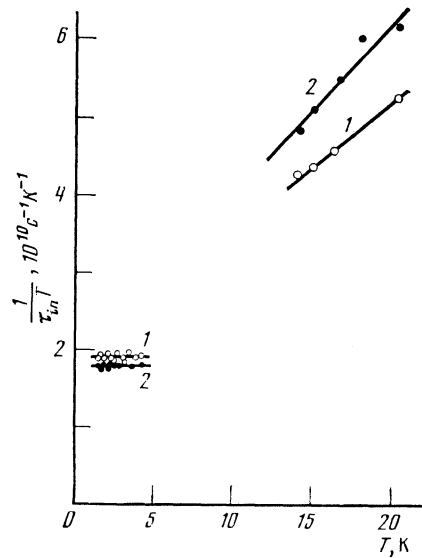


FIG. 7. Temperature dependences of $(\tau_\varphi T)^{-1}$ for Sb films with $L = 85$ Å (curve 1) and 89 Å (2).

$$\tau_\varphi^{-1} = \pi (kT)^2 / 8\hbar \mathcal{E}_F. \quad (9)$$

The temperature dependence of the time phase relaxation due to inelastic scattering processes can thus be represented as

$$\tau_\varphi^{-1} = AT + BT^2,$$

where A and B are described by expressions (7) and (9). The plot of $(\tau_\varphi T)^{-1}$ vs T should be a straight line with an ordinate intercept A and a slope B . Figure 7 shows such plots for samples with $L = 85$ and 89 Å. The experimental points lie on the expected curve at $T > 14$ K, whereas at helium temperatures $(\tau_\varphi T)^{-1}$ is independent of T . This indicates that the term (9) with T^2 makes no contribution at helium temperatures. The ordinate intercept (the coefficient A) agrees well with (7). The slope of the line for hydrogen temperatures is $B = 1.6 \cdot 10^9 \text{ s}^{-1} \text{ K}^{-2}$ ($L = 85$ Å) or $2.2 \cdot 10^9 \text{ s}^{-1} \text{ K}^{-2}$ ($L = 89$ Å). An estimate of the coefficient B of T^2 in (9) yields $3.5 \cdot 10^9 \text{ s}^{-1} \text{ K}^{-2}$, i.e., close to the experimental value. It must be noted, however, that Eq. (9) does not contain the experimentally observed dependence on the sample resistance, i.e., on the film thickness. If we recognize, that \mathcal{E}_F in thin films can increase with decreasing thickness because of the anomalous size effect,¹ a $\tau_\varphi(L)$ dependence can appear in Eq. (9). What is strange in this case is the absence of a contribution with T^2 at $T < 4.2$ K.

The electron-phonon mechanism of electron relaxation is described by the following expressions, depending on the dimensionality of the system¹⁶ at³ $T \ll \Theta_D$

$$\tau_{eph} \sim \frac{1}{\mathcal{E}_F \tau} \frac{\Theta_D^3}{T^4} \quad 3D \text{ phonons.} \quad (10)$$

$$\tau_{eph} \sim \frac{1}{\mathcal{E}_F \tau} \frac{\Theta_D^2}{T^3} \quad 2D \text{ phonons.} \quad (11)$$

The wavelength $\lambda_{ph} = 2\pi^2 \hbar v_{ac} / kT$ of the acoustic phonon can be estimated, viz., $\lambda_{ph} \gtrsim 10^{-8} \text{ cm} \gtrsim L$ at $T < 4.2$ K and $\lambda_{ph} < 5 \cdot 10^{-7} \text{ cm} < L$ at $T > 10$ K. That is to say, $3D$

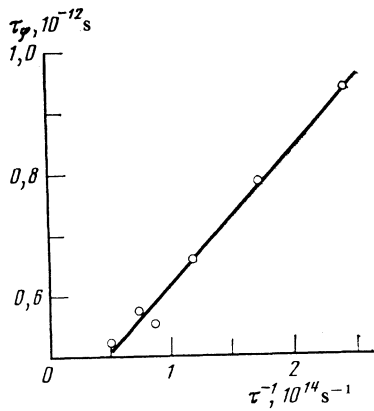


FIG. 8. Dependence of τ_{ϕ} on the reciprocal relaxation time τ^{-1} at 20 K.

phonons are present in these films at hydrogen temperatures, whereas at helium temperatures there are no 3D phonons and the phonon spectrum is determined by the acoustic matching of the film to the glass substrate.

In connection with the features of the Fermi surface in semimetals (small Fermi momentum of the electrons in the C_2 and C_3 directions), an important role in electron-phonon scattering is played by the effective Debye temperature Θ_D^{eff} at which the phonon momentum becomes comparable with the Fermi momentum in the C_2 and C_3 directions. For antimony estimates yield $\Theta_D^{\text{eff}} \approx 10$ K (≈ 1 K for Bi). At temperatures $T > \Theta_D^{\text{eff}}$ the exponent in the $\tau_{\text{eph}}(T)$ dependence should decrease. A $\tau_{\text{eph}} \propto T^{-2}$ dependence was observed in antimony in measurements of the amplitude of the rf size-effect line.¹⁷

The value of τ_{ϕ} at 20 K is proportional to $1/\tau$, the reciprocal elastic-relaxation time (Fig. 8). Thus, the relations $\tau_{\phi} \propto T^{-2}$ and $\tau_{\phi} \propto 1/\tau$, as well as the absence of such a contribution at helium temperature, given grounds for concluding that at hydrogen temperatures the decisive inelastic-relaxation mechanism in antimony in electron scattering by 3D phonons. At helium temperatures we have $\lambda_{\text{ph}} < L$, i.e., this mechanism does not work in this region. The $\tau_{\phi} \propto T^{-1}$, τ dependence at 1.5–4.2 K is connected with the EEI.

CONCLUSION

The measurements of the temperature and magnetic-field dependences of the electric resistance of thin antimony films have shown that a significant role in the conductivity of disordered films 80–150 Å thick is played by effects of weak localization and interaction of the electrons. The quantum interference corrections to the $\Delta\sigma(T)$ dependence are due both to localization and to interaction, so that by measuring

the $\Delta\sigma(T)$ dependence in a magnetic field one can separate the WL and EEI contributions in the diffusion channel.

The magnetic field dependence of $\sigma(H)$ at various temperatures is connected with WL effects. Analysis of this dependence made it possible to determine in experiment the electron inelastic-relaxation time and to study the possible energy-relaxation mechanisms at various temperatures in disordered antimony films.

The authors are grateful to Yu. F. Komnik for constant interest in the work, and the B. L. Al'tshuler, A. I. Kopelovich, and L. A. Pastur for a helpful discussion of the results.

¹That this is precisely the case in the films which have been investigated follows from the data on the magnetoconductance of the films¹¹ and will be discussed below.

²In bismuth, too, $\tau_{\phi}(T)$ went from being proportional to T^{-1} at $T < 1$ K to being proportional to T^{-2} at $T > 4$ K (Ref. 8).

³The applicability of these equations to the investigated antimony films is limited, since the electron wavelength, the mean free path, the film thickness, and the phonon wavelength are all quantities of the same order.

⁴Yu. F. Komnik, E. E. Bjukhshtab, Yu. V. Nikitin, and V. V. Andreevskii, Zh. Eksp. Teor. Fiz. **60**, 669 (1971) [Sov. Phys. JETP **33**, 364 (1971)].

⁵V. V. Andrievskii, A. V. Butenko, and Yu. F. Komnik, in: Fizika kondens. sost. (Condensed-State Physics), Physicotech Inst. for Low Temperatures, Ukr. Acad. Sci., 1974, No. 32, pp. 45–55.

⁶Yu. F. Komnik and V. V. Andrievskii, Fiz. Nizk. Temp. **1**, 104 (1975) [Sov. J. Low Temp. Phys. **1**, 51 (1975)].

⁷E. I. Bukhshtab, Yu. F. Komnik, and Yu. V. Nikitin, Fiz. Tverd. Tela (Leningrad) **15**, 2212 (1973) [Sov. Phys. Solid State **15**, 1475 (1974)].

⁸B. L. Al'tshuler, A. G. Aronov, A. I. Larkin, and D. E. Khmel'nitskii, Zh. Eksp. Teor. Fiz. **81**, 768 (1981) [Sov. Phys. JETP **54**, 411 (1981)].

⁹B. L. Altshuler and A. G. Aronov, Electron-Electron Interaction in Disordered Conductors. Modern Problems in Condensed Matter, North-Holland, 1985.

¹⁰Yu. F. Komnik, E. I. Bukhshtab, A. V. Butenko, and V. V. Andrievskii, J. Low Temp. Phys. **52**, 317 (1983).

¹¹F. Komori, S. Kobayashi, and W. Sasaki, J. Phys. Soc. Jpn. **52**, 368 (1983).

¹²Yu. F. Komnik, E. I. Bukhshtab, A. V. Butenko, and V. V. Andrievskii, Sol. St. Commun. **44**, 865 (1982).

¹³A. K. Savchenko, A. S. Rylik, and V. N. Lutskii, Zh. Eksp. Teor. Fiz. **85**, 2210 (1983) [Sov. Phys. JETP **57** (1983)].

¹⁴A. V. Butenko, E. I. Bukhshtab, and Yu. F. Komnik, Fiz. Nizk. Temp. **9**, 100 (1983) [Sov. J. Low Temp. Phys. **9**, 52 (1983)].

¹⁵V. I. Beletskii, A. V. Golik, A. P. Korolyuk, and M. A. Obolenskii, Zh. Eksp. Teor. Fiz. **69**, 1045 (1975) [Sov. Phys. JETP **42**, 531 (1975)].

¹⁶N. B. Brandt, N. Ya. Minima, and Chu-Chen-Han, *ibid.* **51**, 108 (1966) [**24**, 73 (1967)].

¹⁷B. L. Altshuler, A. G. Aronov, and D. E. Khmel'nitskii, J. Phys. C **15**, 7367 (1982).

¹⁸E. Abrahams, P. W. Anderson, P. A. Lee, and T. V. Ramakrishnan, Phys. Rev. **B24**, 6783 (1981).

¹⁹M. E. Gershenzon, V. N. Gubankov, and Yu. E. Zhuravlev, Zh. Eksp. Teor. Fiz. **85**, 287 (1983) [Sov. Phys. JETP **58**, 162 (1983)].

²⁰V. F. Gantmakher and V. T. Dolgoplov, *ibid.* **60**, 2260 (1971) [**33**, 1215 (1971)].

Translated by J. G. Adashko